The Role of Inhaled Particles in the Pathophysiology of Cardiovascular Disease

Final Report

Agreement No. 04-320

Michael Kleinman, Principle Investigator
Department of Medicine
University of California, Irvine
Irvine, CA 92697-1825

Revised 3 May 2010

Prepared for the California Air Resources Board and the California Environmental Protection Agency

Disclaimer

The statements and conclusions in this Report are those of the contractor and not necessarily those of the California Air Resources Board. The mention of commercial products, their source, or their use in connection with material reported herein is not to be construed as actual or implied endorsement of such products.

Acknowlegements

This project was a joint effort of Air Pollution Health Effects Laboratory at the Department of Medicine, UCI and the Institute of Environmental Medicine at New York University. At UCI I want to acknowledge the technical efforts of Dr. Dianne Meacher, Dr. Katherine Osann, Glenn Gookin, Paul Willett, Michael MacKinnon and Karina Salazar for the exposure, the chemical and biochemical assays and the data analyses on which this project depended. At NYU I want to thank Drs. Morton Lippmann, Lung Chi Chen and Terry Gordon who helped in the overall study design, data analysis and for the extraordinary support of this project by supplying the equipment and personnel for performing the ultrasonic microscopy used in this study. The NYU efforts were part of projects supported by the NYU Particle Center which was funded by the USEPA. I also want to thank Charles Bufalino at UC Riverside who acted as our site liaison for the exposure activities that we were able to conduct at UCR. This Report was submitted in fulfillment of ARB Agreement No. 04-320, "*The Role of Inhaled Particles in the Pathophysiology of Cardiovascular Disease"* by The Regents of the University of California, Irvine under the partial sponsorship of the California Air Resources Board. Work was completed as of February 2009.

Table of Contents

The Role of Inhaled Particles in the Pathophysiology of Cardiovascular Disease i

Final Report i

Disclaimer ii

Acknowlegements ii

Table of Contents iii

List of Figures vi

List of Tables vii

List of Inventions viii

List of Copyrighted Materials viii

List of Terms, Abbreviations and Symbols ix

Abstract xi

Executive Summary xii

Background xii

Methods xii

Results xiii

Conclusions xiii

Introduction 1

Methods and Materials 2

Experimental Techniques 2
Selection and Characteristics of the Animal Model 2
Animal Husbandry 3
Ambient Particle Concentrator 3
Exposure Chambers 3
Exposures 4
Exposure Procedure 5
Bioassay and Data Analysis Methods 8
Analyses of Lung Lavage and Tissue Specimens 8
Lung Histology 9
Inflammatory and anti-inflammatory cytokines and markers of vascular inflammation 10
Details of implanting the Electrocardiography (ECG) telemetry device 11
Ultrasonic Microscopy 14
Results 14
CAPs ($PM_{2.5}$) Concentrations during the 6-Month Study Period 14
Lavage Fluid Analyses 15
Atherosclerosis Development after CAPs Exposure 17
Histologic Assessment of Lesion Burden 20

ECG Assessments 21

Biomarkers of Systemic and Vascular Inflammation 26

Summary of NYU Findings (Sun et al. 2005) 30

Conclusions 30

References: 33

List of Figures

Figure 1. Schematic Diagram of VACES and Exposure System 1

Figure 2. Elemental and Organic Components in the Exposure Atmospheres..... 15

Figure 3. Ultrasound Image of a Mouse Aorta, in vivo 17

Figure 4. Changes in Plaque Thickness and Percent Lumen Area after 2 and 4 months of exposure in 16 control and 16 CAPs-exposed mice. 19

Figure 5. Typical Oil Red-O and hematoxylin counterstained sections used for histologic assessment of plaque areas..... 20

Figure 6. Heart Rates in Mice During and After Exposure During a 6-month Study 22

Figure 7. Changes in Heart Rate Variability During a 6-month Study..... 23

Figure 8. Normal ECG Tracing Showing Typical P,Q,R,S and T Waveform..... 24

Figure 9. ECG from CAPs-exposed Mouse Showing ST-segment Depression 24

Figure 10. Changes in Fraction of Monitoring Periods with ST Changes..... 26

Figure 11. Relationship between Plaque Formation Measured Ultrasonically and Plasma CRP (n=16/group) 29

List of Tables

Table 1. Cell Counts and Cell Differentials (mean ± se) 16

Table 2. Cytokines in Bronchoalveolar Lavage Fluid (pg/mL; Mean ± se) 16

Table 3. Bracheocephalic Artery Plaque Wall + Plaque Thickness (Mean ± se) 18

Table 4. Plaque Measured Histologically in Samples of the Aortic Arch (Mean ± se) 20

Table 5. Biomarkers of Systemic and Vascular inflammatory Processes (ng/mL Plasma) 27

Table 6. Protein Carbonyls in Aortal Tissue 28

List of Inventions

None

List of Copyrighted Materials

None

List of Terms, Abbreviations and Symbols

Symbol or Abbreviation	Explanation
AAALAC	Association for the Assessment and Accreditation of Laboratory Animal Care
APHEL	Air Pollution Health Effects Laboratory, University of California, Irvine
apoE-/-	Mice in which the gene regulating apoE is knocked out
AQMD	Southern California Air Quality Management District
Arteriosclerosis	A chronic disease in which deposits of cholesterol and/or calcium cause abnormal thickening and hardening of the arterial walls with resulting loss of elasticity
Atherosclerosis	A stage of arteriosclerosis in whichfatty deposits (atheromas) form inside the arterial walls, thus narrowing the arteries
Atherothrombosis	Disruption of an atherosclerotic plaque or lesion resulting in release of fragments that can block an artery
BAL	Bronchoalveolar Lavage
CAPs	Concentrated Ambient Particles
CO	Carbon Monoxide
CRP	C-reactive protein (acute phase protein which is a marker of systemic inflammation)
CVD	Cardiovascular disease
EC	Elemental Carbon
ECG	Electrocardiogram
E-selectin	Endothelial cell adhesion molecule
HEPA	High Efficiency Particle Air filter

ICAM	Intercellular Cell Adhesion Molecule
NO2	Nitrogen Dioxide
NYU	New York University
O3	Ozone
OC	Organic Carbon
PAI-1	Plasminogen activation inhibitor
PM	Particulate matter
PM2.5	Particulate matter less than 2.5 μm in aerodynamic diameter
PTFE	Fluorocarbon-based filter media
SO2	Sulfur Dioxide
SS	Stainless Steel
UFP	Ultrafine Particles
VACES	Versatile Aerosol Concentration Enrichment System
VCAM	Vascular Cell Adhesion Molecule
μg/m3	Micrograms per meter cubed
μm	Micrometer

Abstract

Mice that were genetically susceptible to developing atherosclerosis were fed a normal chow diet and were exposed to about 160 μg/m^3 fine particle air pollution ($PM_{2.5}$) for 4 days per week, 6 hours per day for 6 months in Riverside, CA. Control mice were exposed to purified air. The goal of this study was to determine if exposure to pollutant particles would accelerate the development of atherosclerosis in these mice and if the exposures also caused increased evidence of heart dysfunction. The development of atherosclerotic plaque was followed during the experiment using a non-invasive ultrasonic microscope method and a subset of mice was equipped with a telemetry device that relayed their electrocardiograms to a computer. We examined several factors relevant to mechanisms of development of atherosclerosis and heart disease. At the end of the six month exposure we measured the development of plaque in the aorta of each mouse and also measured several biomarkers in serum that are known to be elevated in humans with coronary artery disease. After six months of exposure to elevated levels of $PM_{2.5}$ there was, on average, a 60% increase in the amount of plaque in the arteries of these mice than there was in the air-exposed mice. Although there was substantial animal to animal variation, this finding was significant ($p \leq 0.05$). The level of C-reactive protein, which is one indicator of systemic inflammation, was positively associated with the development of plaque in the CAPs-exposed mice, but not in the air-exposed mice. The conclusion drawn from this study is that exposure to particulate pollution ($PM_{2.5}$) in California significantly accelerates atherosclerosis development.

Executive Summary

Background

The mechanisms by which particulate matter (PM) exposure disrupts cardiac function and worsens cardiovascular disease (CVD) are not well understood. There is a growing body of knowledge that suggests that PM exposure can induce inflammatory changes in blood vessels and exacerbate atherogenesis leading to the development of atherosclerotic plaques and lesions. We hypothesized that PM exposure would abnormally activate endothelial cells and induce vascular inflammation that will lead to the accelerated formation of arterial plaques which are a hallmark of atherosclerosis.

Methods

The study was performed using mice that were genetically susceptible to the development of atherosclerosis. The mice were exposed to concentrated ambient fine particles ($PM_{2.5}$) for 4 days per week, 6 hours per day for 6 months. The exposure concentrations averaged about 160 $\mu g/m^3$. We examined several factors relevant to mechanisms of atherogenesis and the development of cardiovascular heart disease. The development of atherosclerosis was monitored over the course of exposures using an ultrasound microscope technique. Mechanistic endpoints that were evaluated included plasminogen activation inhibitor-1 (PAI-1), which is an acute-phase reactant that can become transiently elevated by inflammation and plays a role in atherothrombosis; soluble forms of the intercellular, vascular and endothelial cell adhesion molecules ICAM-1, VCAM-1 and E-selectin, that are postulated to play a role in development of atherosclerotic plaque; matrix metallopeptidase-9 which is involved in tissue remodeling associated with inflammatory disease processes; and C-reactive protein, which is produced in the liver and is an acute phase proteins that increase during systemic inflammation. In addition, we measured the effects of exposure on cardiac function in a subset of the mice that were implanted with cardiographic transponders. Heart rate, heart rate variability and arrhythmias were determined. Frozen samples of aortic arch were

reserved for analysis of biomarkers associated with oxidative stress including defensive molecules (glutathione and heme-oxygenase) and for protein carbonyls as a measure of oxidative damage.

Results

The results of this study show that $PM_{2.5}$ exposure (160 μg/m^3) accelerated the development of atherosclerotic plaque in genetically susceptible mice approximately 1.6-fold compared to plaque development in mice exposed to purified air ($p \leq 0.05$). The concentration of CRP in plasma was significantly correlated with plaque development in PM-exposed mice but not in air-exposed mice. It is important to note that the mice used in this study were fed a normal chow diet. We can compare our results with a study using similar methods of exposures and endpoints that were performed using mice exposed in New York that were fed either a standard rat chow diet or a high fat (so-called Western) diet by researchers at New York University. In contrast to our study of mice exposed to ambient air in Riverside, CA, the NYU study showed significant results only for the mice fed a high fat diet. It is not possible to rule out that the reason that we observed a significant PM-related increase in atherosclerosis development in mice fed a normal diet while significant PM-related effects were seen in the high fat group in the NYU study was that a higher PM concentration was used in our study (160 μg/m^3) than in the NYU study (85 μg/m^3).

Conclusions

We conclude that subchronic exposure to elevated concentrations of $PM_{2.5}$ will potentiate the development of atherosclerosis. An earlier study at NYU demonstrated significant increases in plaque formation in genetically susceptible mice after exposure to concentrated $PM_{2.5}$ compared to mice exposed to purified air. In general our results confirm those of this earlier NYU study, however the mice in our study were fed a standard chow diet whereas the NYU group showed significant changes only in mice fed a high fat diet. This might be due to differences in the sources of air pollution between New York and Riverside, CA. We also demonstrated that C-reactive protein in plasma,

which is an indicator of systemic inflammation, may be a useful biomarker for risk of development of atherosclerosis.

Introduction

Heart disease is the leading cause of death in the U.S. Recent data have indicated that exposure to air pollutants is a risk factor and may represent an important preventable cause of both morbidity and mortality among populations living in polluted environments. There are strong and relatively consistent associations between cardiovascular morbidity and mortality and oxidative stress associated with inflammation. Ultrafine particles are capable of inducing the greatest amount of pulmonary inflammation per unit of PM mass. This is thought to be due to the physical and chemical characteristics of ultrafine particles, including, high particle number, high pulmonary deposition efficiency, and a surface chemistry involving a high surface area that can efficiently deliver adsorbed or condensed toxic air pollutants (oxidant gases, organic compounds and transition metals) to the respiratory tract. These toxic air contaminants have all been identified as having pro-inflammatory effects. This research examined the link between particle-induced inflammation and the development of atherosclerosis in normal and atherosclerosis-prone mice. In addition to examining the acceleration of disease during acute and chronic PM exposures, we examined signaling pathways for oxidative stress and inflammation-associated tissue damage to determine the relative importance of these mechanisms in the development or exacerbation of cardiovascular disease. Improved understanding of the roles of these specific mechanisms could lead to improved techniques for preventing or treating heart diseases caused by environmental contaminants. A seminal series of studies performed by Chen, Lippmann and colleagues at New York University (NYU) demonstrated that exposure to concentrated ambient fine ($PM_{2.5}$) particles in Tuxedo NY could exacerbate the development of atherosclerotic lesions in mice that were genetically predisposed to abnormal lipid metabolism (Sun et al. 2005; Sun et al. 2009). Tuxedo NY is a rural area that is generally exposed to regional air pollution but was characterized by relatively small contributions from industrial emissions. NYU planned a follow-on study in New York City which was more impacted by industrial emissions and motor vehicle emission

than was the Tuxedo site. We sought in this study to coordinate a project with NYU using similar exposure methods and biological endpoints to determine whether exposures to ambient aerosols in the Los Angeles air basin (which is heavily dominated by motor vehicle emissions) would be more atherogenic than was the ambient PM in New York City or Tuxedo NY.

Methods and Materials

Experimental Techniques

Selection and Characteristics of the Animal Model

The transgenic mouse model of cardiovascular disease that we proposed to use in this study was developed from the C57BL/6 mouse. The C57BL/6 strain was has been shown to be particularly susceptible to adverse pulmonary effects from a variety of inhaled substances including O_3 (Kleeberger et al. 2000), acid-coated carbon particles (Ohtsuka et al. 2000) and ovalbumin (Morokata et al. 1999). We originally proposed study to use a knock-out mouse lacking apolipoprotein E (apoE-/-) as well as a double knock-out mouse strain lacking both the apolipoprotein E and the low density lipoprotein receptor (apoE-/-LDLr-/-). However, before we began our project, NYU determined that they would not continue to study the double knock-out strain because they had a severely abbreviated life span and were subject to serious skin lesions. Both we, and NYU, therefore focused only on the single knockout apoE-/- mouse model.

Progression of coronary artery disease in the mice was originally to be monitored over the course of the study solely with implanted ECG transmitters. Animals were to be euthanized after specific times of exposure so that histological assessments of plaque size could be determined. With the assistance of NYU, however, a novel ultrasonic microscope method was developed which permitted us to non-invasively assess plaque development so that animals could be exposed chronically.

Animal Husbandry

Animals were housed two to a cage in AAALAC accredited animal housing facility at the Air Pollution Health Effects Laboratory (APHEL). The mice that were implanted with telemetry devices were housed singly so that ECG parameters could be monitored while the mice were in the vivarium. Animals were provided with a normal chow diet (Harlan Teklad) and water ad libitum.

Ambient Particle Concentrator

Ambient particles with particle diameters smaller than 2.0 μm were concentrated using the Versatile Aerosol Concentration Enrichment System (VACES) which has been described in detail by Kim et al. (Kim et al. 2001a; Kim et al. 2001b). VACES consists of a size selective ($PM_{2.5}$) inlet, a saturator/chiller module that supersaturates the aerosol with water vapor causing fine and ultrafine particles to grow to a size that can be inertially separated using a virtual impactor, and a diffusion drier module that removes the excess water vapor and returns the aerosol to a size distribution that is very close to that in the unconcentrated ambient air. The system is mobile and capable of enriching the concentration of particles in the range of 0.03- 2.0 μm by up to a factor of 30 x ambient, depending on the output flow rate (Kim et al. 2000a). The efficiency of concentration begins to fall off above 2.0 μm or below 0.03 μm.

Exposure Chambers

A whole-body exposure mouse chamber was designed specifically for use with the VACES. Each stainless steel (SS) chamber (20 inches X 12 inches X 6 inches) was segmented into 18 cubicles (1 mouse per cubicle) separated by perforated SS sheets (0.078" Hole Diameter. 36% Open, Staggered, (McMaster-Carr, New Brunswick, NJ). Concentrated ambient particles (CAPs) were delivered through SS particle delivery tubes that distributed CAPs uniformly throughout the exposure chamber (Oldham et al. 2004). A raised sub-floor constructed from perforated SS sheet (0.25” hole Diameter, 50% open, staggered) was used, which permitted urine and feces to fall to the bottom of the vat and kept the mice relatively clean. The exposure atmosphere was exhausted from below the

sub-floor through 2 SS tubes, each 40 cm in length with 28 0.5 mm downward-facing holes. Absorbent sheets impregnated with an antibiotic to prevent fecal bacteria from generating ammonia from urine are placed under the exhaust tubes to absorb urine and to collect feces.

Exposures

Thirty-two mice were exposed to fine CAPs (particles of physical diameters smaller than 2.5 μm), which was consistent with the experimental design used by the NYU group (Maciejczyk et al. 2005). Thus, our experiment was performed in a way so as to facilitate comparison between the NY and California studies. Total group sizes were Air = 16 and CAPs = 16. Eight mice in each group were implanted with transponders to obtain heart rate and electrocardiograph data. The remaining 8 in each group were used for histology and bronchoalveolar lavage studies.

Exposures were conducted at the University of California, Riverside (UCR) from June 2006 to December 2006. Riverside, CA is a site at which aerosol concentrations are among the highest in the U.S. In addition, detailed data are available on the chemical and physical characteristics of the pollutant components present. The South Coast Air Quality Management District (AQMD) provided data obtained at a site relatively near to our Riverside site. Those data included 1-hr averages of mass concentrations of $PM_{2.5}$, PM10, and concentrations of criteria gases including O_3, NO_2, CO and SO_2. During exposures, we monitored concentrations of ambient and CAPs particles. Samples were also collected on pre-fired quartz filters which were composited on a weekly basis and analyzed for elemental carbon (EC) and organic carbon concentrations (OC). EC is a reasonable tracer for particles originating from diesels and represents between 5 - 20% of the UFP at the Riverside site. EC and OC were measured by a thermal photometric method on a fraction of the filter; the remaining fractions were stored (-80º C) for future analyses. If OC is determined to predict acute or chronic adverse cardiac responses, we will evaluate the possibility of performing more detailed organic analyses. Particles were also collected for mass concentration and chemical analyses on pre-weighed PTFE filters.

Following collection, the filters were equilibrated overnight at constant humidity and weighed. These filters were submitted to NYU for analysis of metals by X-ray fluorescence - Fe, V, Zn, Cr, Ni, Cu, Pb and Mn. These metals were selected because previous inhalation or in vitro studies have shown them to be potentially toxic (Campen et al. 2001; Carter et al. 1997; Ghio et al. 1999; Hlavay et al. 2001; Lippmann et al. 2006; Magari et al. 2002; Natusch et al. 1974). The trace element analyses are in progress.

Exposure Procedure

Animals were housed at UC Irvine (UCI), transported daily to Riverside and exposed to CAPs at the UCR field location in a specially configured exposure trailer. At UCI the mice were housed in ventilated caging attached to an air purification system. The air purifier delivered filtered air at flows adequate to provide 15-20 air exchanges per hour in each ventilated cage unit. The vivarium is supplied with Class 100 filtered air using a laminar flow air purifier that consists of a 1000 CFM blower, an oxidizing adsorbent canister containing permanganate-impregnated alumina spheres, and a high efficiency particle air (HEPA) filter system. Between exposures the animals were supplied with purified air, clean water and a normal chow diet (Harlan Teklad), ad lib. During exposures, the animals were placed into sealed, compartmentalized exposure chambers and were exposed to fine concentrated ambient particles (CAPs) for 6 hours per day. Control animals received purified air under conditions identical to those of the animals exposed to CAPs. Temperature was monitored continuously during the exposures and held to 75 ± 5 °C. Animals were observed throughout the exposure period for signs of distress. The Versatile Aerosol Concentrator for Exposure Studies (VACES) designed by Sioutas and colleagues at USC (Kim et al. 2000a; Kim et al. 2001a; Kim et al. 2001b; Kim et al. 2000b; Sioutas et al. 1999) has been used by UCI for exposures of mice near freeways in Los Angeles (Kleinman et al. 2005). The VACES was purchased from the University of Southern California and was rigorously tested in Riverside and then coupled to our exposure chambers. The concentrator has the capability to use 3 independent virtual impactors (VI's) to concentrate particles in the ultrafine, fine and

coarse particle size ranges. A schematic of the VACES and exposure system is shown in Figure 1.

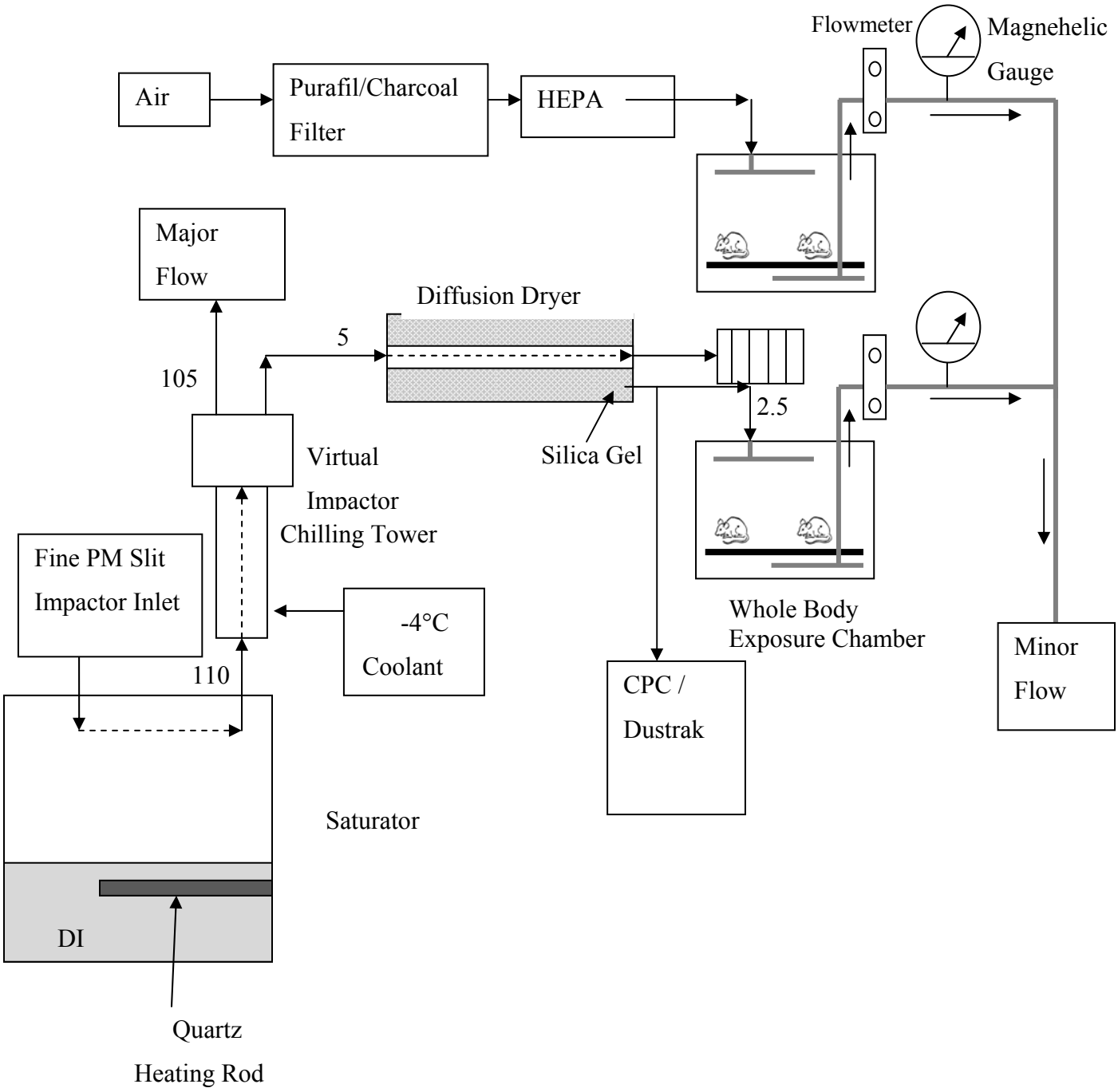

Figure 1. Schematic Diagram of VACES and Exposure System

We determined concentration efficiency and losses in particle transmission between the VI and the exposure chamber. Particle concentrations were measured as a function of particle size before concentration, after concentration and after passage through the exposure chamber using a Climet optical particle size monitor (Climet Instruments, Redlands, CA). The measured concentration factors were 20 to 30% lower than those estimated based on the nominal flow rates or compared to published performance data for a coarse particle concentrator (Chang et al. 2002). We estimate that there are some losses due to the chamber configuration and flow baffles placed into the exposure system to provide relatively uniform particle distributions during the exposures. We performed flow distribution measurements and modified the configuration as necessary to reduce particle losses in the system prior to initiating the study.

Bioassay and Data Analysis Methods

Blood: serum samples were collected from each animal from the descending aorta for cytokine and circulating biomarker levels.

Lungs: one side of the lung was lavaged (see below) and snap frozen for gene expression analysis. The other side of the lung was fixed in buffered formaldehyde at a fixed pressure for subsequent morphometric analysis.

Heart: A sample of the heart was collected and frozen for subsequent gene expression analyses. The remaining tissue was fixed for subsequent morphological study.

Analyses of Lung Lavage and Tissue Specimens

Bronchoalveolar Lavage (BAL). Mice were anesthetized by intraperitoneal injection of sodium pentobarbital. The abdominal aorta was severed, and a polyethylene catheter was placed in the trachea and tied in place. An incision was made in the diaphragm to allow

lung expansion during the lavage. Lungs were lavaged by introduction of 0.025 ml/g body weight HEPES buffered Hanks Balanced Salt Solution (HBSS) without Ca^{+2} or Mg^{+2} through a tracheostomy tube, followed by withdrawal of the fluid. The process of introduction and withdrawal was repeated three times and 0.5 ml of lavage fluid was transferred to a 1.5 ml polypropylene centrifuge tube. The lavage was repeated two additional times; the fluid from the last two lavages was pooled in a separate centrifuge tube. The lavage fluid from each animal was centrifuged at 800 x g for 10 min to isolate cells and the cell-free centrifugate was frozen for subsequent analysis.

Total cell number was determined by hemocytometry. Viable cells were differentiated from non-viable cells by trypan blue exclusion. An aliquot representing 100,000 cells was placed on a microscope slide using a cytocentrifuge and stained with a Wright-Giemsa preparation. Differential cell counts were made by microscopically examining a minimum of 300 cells per sample. Lung lavage fluid was frozen and reserved for analysis of cytokines/chemokines involved in pulmonary inflammation, i.e., Interleukin-6 (IL-6), KC (a member of the CXC chemokine family that includes inflammatory cytokines IL-8 and GROα), and Tumor Necrosis Factor-α (TNFα).

Rouse and colleagues reported that gene array analyses on lavaged lung tissues revealed elevation of genes related to oxidative stress and lung injury (Rouse et al. 2008). It is possible that lavaging might affect subsequent gene analyses if, for example, lavaging induced more infiltration of inflammatory cells in one group than the other. However that was not the case in this study and mice and tissue from both control and exposed mice were treated identically so that differences between the groups should still be relevant. The frozen lung tissues from our study have been stored for subsequent gene expression analyses for cardiovascular biomarkers.

Lung Histology

The trachea and right lung were fixed by airway instillation of 4% paraformaldehyde at a pressure of 20 cm H_2O, and the tissue transferred to 70% ethanol after 24 hours. The total volume of the fixed lung was measured by volume displacement. The right upper

lobe was paraffin-embedded, sectioned and stained with hematoxylin and eosin and reserved for histopathology analyses.

Vascular and Cardiac Histology

All morphological assessments were done blind (i.e. without knowledge of the treatment group). At sacrifice, the mice were euthanized with an overdose of pentobarbital and the heart and aorta perfused with 4% paraformaldehyde. The heart and thoracic and abdominal aorta were removed en bloc. Sections of the aorta were obtained from the proximal, central and distal areas, snap frozen and stored in liquid nitrogen. These samples were homogenized and used for assays of gene expression, and for analyses of biomarkers of vascular inflammation and oxidative stress. The remaining proximal and distal aorta segments were cut longitudinally. One section was frozen in O.C.T. embedding medium (Sakura Finetek, Torrance, CA) and reserved for subsequent laser capture microdissection and genomic and proteomic analysis. The remaining aorta sections were fixed in buffered formaldehyde and examined for total atherosclerotic lesion areas, lipid contents, and cellularity (Wadsworth et al. 2002). A section of the heart was removed, snap-frozen in liquid nitrogen and reserved for gene expression analysis. The remaining tissues were fixed in 4% paraformaldehyde and stored for future histological analysis.

Inflammatory and anti-inflammatory cytokines and markers of vascular inflammation

Samples of blood plasma were analyzed using a state of the art multiplexed bead assay system (Luminex). The system uses fluorescently tagged beads to which antibodies to specific proteins are attached. After incubation with the sample, the beads are incubated with detection antibodies and then analyzed using a fluorescent flow sorting system (similar in working principle to flow cytometry) and the data are recorded and quantified using an online computer. A custom assay set that analyzes protein biomarkers associated with vascular inflammation and oxidative stress was used and included: plasminogen activation inhibitor-1 (PAI-1), which is an acute-phase reactant

that can become transiently elevated by inflammation and plays a role in atherothrombosis; soluble forms of the intercellular, vascular and endothelial cell adhesion molecules ICAM-1, VCAM-1 and E-selectin, that are postulated to play a role in development of atherosclerotic plaque; matrix metallopeptidase-9 which is involved in tissue remodeling associated with inflammatory disease processes; and C-reactive protein, which is produced in the liver and is an acute phase proteins that increase during systemic inflammation. Samples of BAL and frozen aorta tissue were reserved for analyses of inflammatory/anti-inflammatory cytokines (TNF-α, IL-6, IL-8) using the Luminex system. Aortal arch and descending aorta tissue was analyzed for malonaldehyde (MDA) and protein carbonyls as markers of oxidative stress, using commercially available kits (Cayman Chemical, Ann Arbor MI).

Details of implanting the Electrocardiography (ECG) telemetry device

This protocol is for the surgical implantation of small transmitting devices used to acquire research data as part of a telemetry system (PhysioTel Telemetry system, Data Sciences International, St. Paul, MN). These devices are designed to measure biopotential (ECG tracings), temperature, and physical activity in mice. The temperature measurements are monitored throughout the study because rodents have a marked diurnal metabolic cycle that influences cardiovascular function. The temperature data are also evaluated to assure that the surgical procedure does not induce elevated core temperatures that might signal a systemic inflammatory reaction. The implantable device which weighs 3.8g and has a volume of 1.75 mL consists of the following major components: (1) device body, and (2) biopotential leads. The device was soaked in sterile saline for 15 min prior to being placed in the peritoneal cavity. This placement has excellent biocompatibility, the ability to measure core temperature, and is relatively insensitive to changes in the ambient temperature. Aseptic techniques were used throughout the implantation procedure. Mouse core temperatures are monitored throughout the study to evaluate potential inflammatory responses in the mice.

Isofluorene was administered via inhalation to anesthetize the mice. Once anesthetized, the animal's eyes were lubricated with a sterile ophthalmic ointment to prevent corneal drying. The body hair of the mouse was shaved using electric clippers (#40 blade) from the ventral abdomen from the subxiphoid area to the pelvis, and the sites of subcutaneous electrode placement. The shaved area was cleaned and disinfected with alcohol and an iodine-based disinfectant. While under general anesthesia, the animals were provided a heat source during surgery from lamp and were covered with a blanket.

A sterile drape impermeable to moisture was adhered tightly to the skin, and a ~1 cm midline abdominal incision was made. The contents of the abdomen were exposed using a retractor. The body of the telemetry device was placed on top of the intestines parallel to the long axis of the body with the catheter directed caudally.

ECG Lead Placement: A skin incision was made at the site of negative lead placement. Using a trocar, a tunnel was made subcutaneously from the abdominal incision to approximately 1 cm beyond the lead incision. A plastic sleeve was slid over the end of the trocar, and the trocar was used to guide the sleeve into the prepared tunnel. The trocar was removed, leaving the sleeve in place. A 14-gauge needle was passed through the abdominal wall lateral to the cranial aspect of the incision going from the outside into the abdominal cavity. One of the leads was passed through the needle and out of the abdomen. The needle was withdrawn leaving the lead externalized. The lead was passed through the waiting plastic sleeve to the desired site, and the sleeve was removed. The silicone coating was removed from the tip of the lead using a sharp sterile blade to expose 1.5 cm of stainless steel wire. A tip cover was screwed onto the exposed wire, leaving at least 1 cm of the wire exposed. The muscle fibers were bluntly dissected at the desired site to provide a shallow area into which the electrode was placed. The lead was secured by suturing the muscle tissue up over the lead using 4-0 non-absorbable suture. These steps were repeated for the positive lead. The device body was secured in place by closing the abdominal incision and incorporating a suture rib on the device into the closure using non-absorbable sutures (4-0) in a simple interrupted pattern. The skin

incision was closed using skin staples. After surgery, the animal was placed into a warm environment and the breathing air was supplemented with additional oxygen. The animal's recovery was monitored until it was fully awake. Analgesia, buprenorphine (.01 - .05 mg/kg subcutaneously every 12 hours for three days) was provided to all animals post surgery. Enrofloxacin (Baytril) 3 mg/kg BW was administered by subcutaneous injection twice per day for 7 days. The animals were allowed to recover for at least 2 weeks after surgery before being introduced to the exposure procedure. There was no evidence of infection or inflammation proximal to the leads at the end of the study.

ECG Data Analysis: The DataQuest A.R.T. system was used to detect, collect and analyze biopotential, body core temperature and activity telemetry signals from each animal. The acquisition program interfaced with a receiver that is tuned to each animal's implanted ECG telemetry device. At the start of our field study, data was sampled each day of exposure for 15 min. before, for 5 min every 30 min during the 6 hour exposure period and 15 minutes post-exposure. As the project progressed, we were able to expand the monitoring to include monitoring overnight while the animals were housed in the vivarium. The acquisition program automatically cycled through the animals, and acquired data in groups of 4 mice at a time. ECG waveforms were stored on a dedicated computer for subsequent analysis. Heart rate was evaluated and the standard deviation of the normal R to R interval (SDNN) was also determined as a measure of heart rate variability (HRV). Analysis of the ECG waveform was used to extract measures of HRV (the magnitude of variance explained (power) in the heart's rhythm across different frequency bands (spectra) of periodic oscillations in heart rate). Portions of these spectra reflect different autonomic influences on heart rate and BP. The high frequency (HF) band (0.15-0.40 Hz) of the heart period power spectrum has been used to estimate cardiac vagal control (Akselrod et al., 1981; 1985). HRV in this band is linked to respiratory influences and has been referred to as "respiratory sinus arrhythmia" (Porges et al., 1986). Heart period oscillations at lower frequencies (LF, 0.04-0.15 Hz) are less well understood. They may represent mixed sympathetic-parasympathetic and thermoregulatory influences (Akselrod et al. 1981; Pomeranz et al, 1985; Saul et al.,

1989; 1991). The numbers of premature atrial and ventricular beats and incidences of ischemia (i.e. ST segment depression) were also determined by analysis of the ECG waveform.

Ultrasonic Microscopy

Ultrasonic microscopy was performed using a VEVO 660 UBM rolling cart developed by VisualSonics, Inc. which was provided and operated for this study by Dr. Chen and his colleagues from NYU. The unit provided a two-dimensional image with a spatial resolution of ~50 μm, with penetration depth of ~20 mm. The NYU investigators used this device to measure arterial cross-sections prior to deploying the animals in the field and at 2 month intervals during exposures. This non-invasive method allowed us to monitor the development of atherosclerotic plaques in the vasculature. In addition we were also able to use Doppler echocardiography to measure hemodynamic parameters such as blood flow and cardiac ejection fraction. These measurements were repeated at 2 to 3 month intervals during the exposures.

Results

CAPs ($PM_{2.5}$) Concentrations during the 6-Month Study Period

The mean ± standard error (SE) concentration of $PM_{2.5}$ CAPs in the exposure chamber was 166 ± 13 $\mu g/m^3$. The mean ± SE concentration factor was 8.7 ± 4. The organic carbon (OC) concentration averaged 50 ± 5 $\mu g/m^3$ and the elemental carbon (EC) concentration averaged 8 ± 6 $\mu g/m^3$. The CAPs mass concentration was approximately twice that measured in the NYU study (Sun et al. 2005).

There was a small amount of OC on the clean air filters which could be due to breakthrough in our air purifiers or slight contamination from handling. However the levels were quite low and were unrelated to the levels of EC (Figure 2). On the other

hand for the exposed filters, there was a proportional increase in OC as a function of EC concentration ($R^2 = 0.34$; $p \leq 0.01$). EC is thought to be a good indicator for diesel and gasoline-fueled engine emissions suggesting that there was a strong contribution of mobile source emissions to the $PM_{2.5}$.

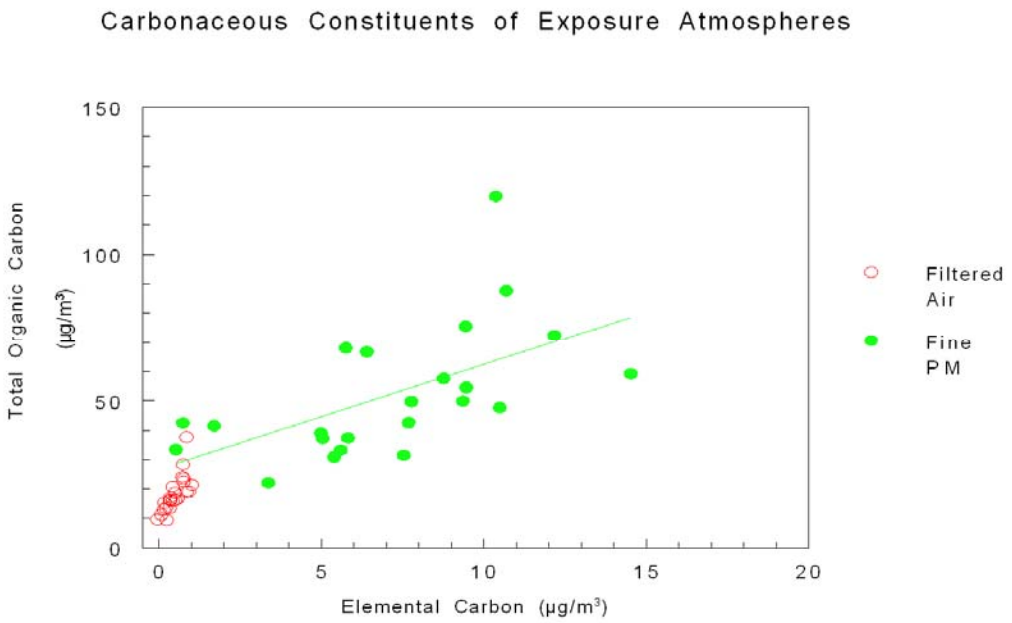

Figure 2. Elemental and Organic Components in the Exposure Atmospheres

Lavage Fluid Analyses

Cell Counts and Differentials: Cells were isolated from the Bronchoalveolar lavage fluid and analyzed for total cells by hemocytometry and viability was assessed by trypan blue exclusion. Stained preparations of the isolated cells were counted and the numbers of macrophages and polymorphonuclear leukocytes (PMNs) were determined. The numbers of lymphocytes and eosinophils were too small to analyze statistically and the PMNs represented about 1% of the viable cells in lavage fluid from both the air-exposed

and CAPs-exposed animals. The data are summarized in Table 1, however there were no statistically significant differences between the groups for any of the parameters.

Table 1. Cell Counts and Cell Differentials (mean ± se)

Parameter	Air (n = 16)	CAPs (n = 16)	p value
Total Cells	63,000 ± 8,000	55,000 ± 8,000	>0.1
Viable Cells	47,000 ±7,000	47,000 ± 7,200	>0.1
Macrophages	46,700 ± 6,900	46,800 ± 7,400	>0.1
PMNs	200 ± 75	580 ± 450	>0.1

The cell-free lavage fluid was analyzed for selected cytokines or chemokines that are known to be associated with lung inflammation. We used a Luminex bead assay system to analyze fluids for KC, IL-6 and TNFα. The levels of IL-6 were below detection limit (2.3 pg/mL) in all of the samples tested. Both KC and TNFα were slightly elevated ($p \leq 0.07$ and $p \leq 0.06$, respectively) in the lavage fluid from CAPs-exposed mice compared to that from air-exposed mice.

Table 2. Cytokines in Bronchoalveolar Lavage Fluid (pg/mL; Mean ± se)

Cytokine	Air (n = 16)	CAPs (n = 16)	P value
KC	4.9 ± 0.3	6.2 ± 0.6	0.07
IL-6	≤ 2.3	≤2.3	
TNFα	15.0 ± 1.3	20.4 ± 2.2	0.06

Atherosclerosis Development after CAPs Exposure

Ultrasonic Imaging: In vivo ultrasonic imaging of atherosclerosis burden in the bracheocephalic artery revealed increasing plaque burden in the mice over the course of the study. This occurred in both air-exposed and CAPs-exposed mice. Data were obtained at baseline and after 2 and 4 months of exposure. Figure 3 shows a typical ultrasonic image from a mouse after 2 months on the exposure protocol. Table 3 summarizes the mean ± SE arterial wall thickness measured in the mice exposed to $PM_{2.5}$ vs the mice exposed to filtered air. Both groups of mice showed significant increases in the wall thickness after 2 and 4 months of exposure, compared to their respective baseline measurements. However, after 2 months the mean difference in wall thickness between the exposure groups was not different. After 4 months of exposure the arterial wall thickness of the CAPs-exposed mice was significantly ($p \leq 0.05$) greater than that of the mice exposed to filtered air.

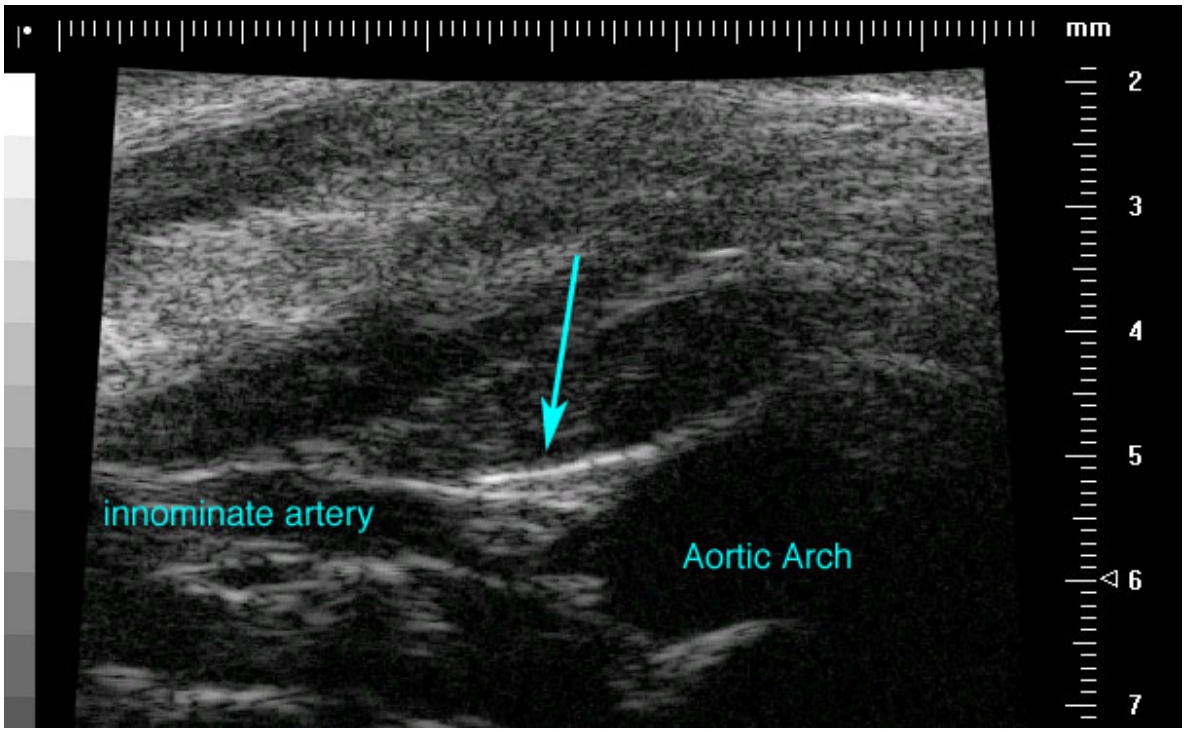

Figure 3. Ultrasound Image of a Mouse Aorta, in vivo

Table 3. Bracheocephalic Artery Plaque Wall + Plaque Thickness (Mean μm^2 ± se)

Exposure	Baseline	2 months	4 months
Air (n = 16)	1226 ±67	2051 ± 67	2794 ± 92
CAPS (n = 16)	1167 ±98	2177 ± 70	3034 ± 58

Figure 4 shows the increase in plaque area from baseline and the decrease in percent lumen area referred to baseline levels. As seen in the figure the plaque area in the CAPs-exposed mice tended to increase with exposure time with a somewhat greater rate of change than did the air-exposed group, as indicated by the slopes of the curves, was greater as well (CAPs, slope = 476, r=0.999; Air, slope =392, r= 0.999). By the end of 4 months of exposure the non-invasively measured group mean plaque area for the CAPs group was slightly, but significantly ($p \leq 0.05$) greater than that of the air-exposed group. The fraction of open lumen decreased for both groups, and although the average % lumen opening was smaller in the CAPs group than in the air group, the differences were not statistically significant.

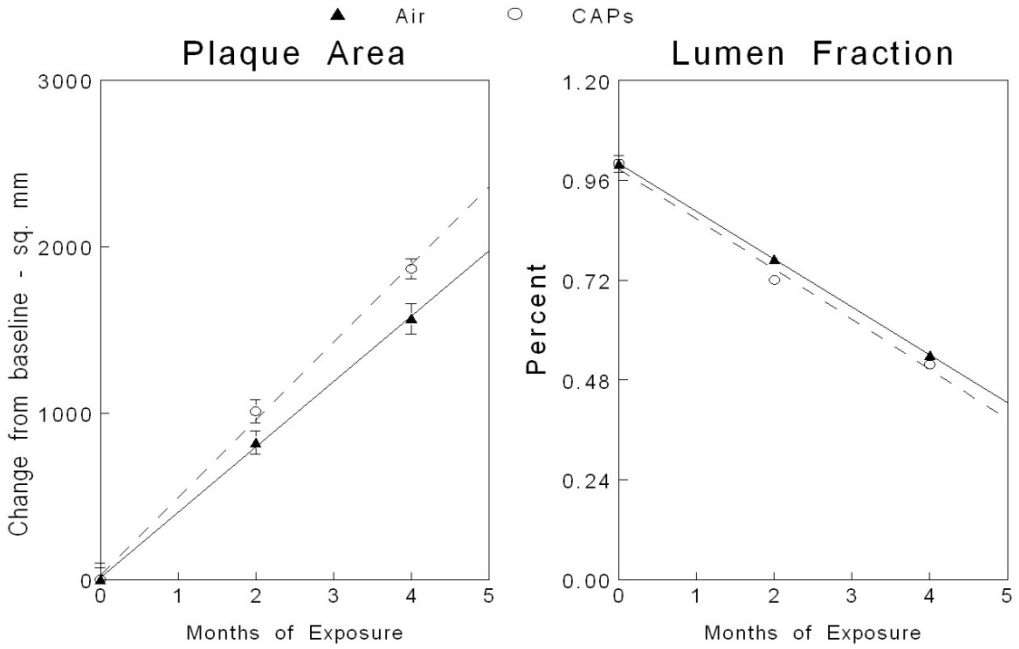

Figure 4. Changes in Plaque Thickness and Percent Lumen Area after 2 and 4 months of exposure in 16 control and 16 CAPs-exposed mice.

Histologic Assessment of Lesion Burden

Figure 5 provides representative sections from morphometric analysis of the aorta in the 2 groups of mice and Table 4 provides estimates of plaque areas identified by staining for lipid content using oil red-O.

Table 4. Plaque Measured Histologically in Samples of the Aortic Arch (Mean ± se)

Atmosphere	N	% Plaque Area
Air	6	4.5 ± 1.9
CAPs	3	7.4 ± 3.4

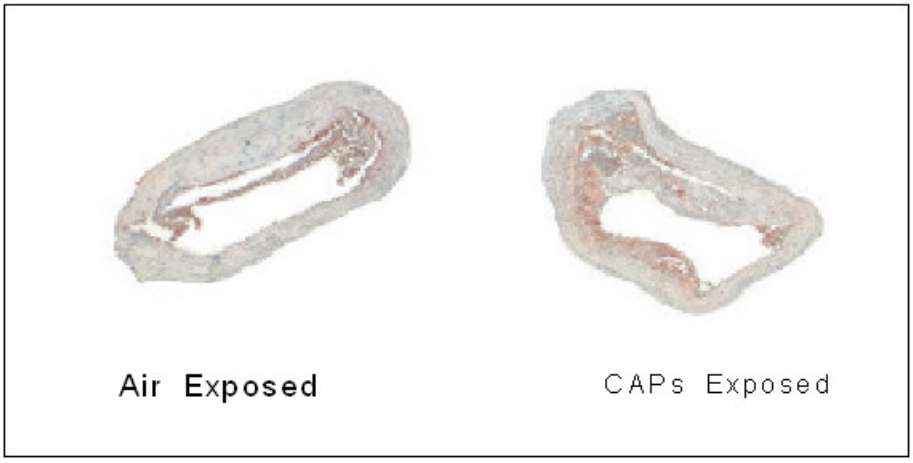

Figure 5. Typical Oil Red-O and hematoxylin counterstained sections used for histologic assessment of plaque areas

ECG Assessments

Heart rates increased significantly when measured during the day in both air-exposed and CAPs exposed mice (solid lines in Figure 6). The rate of increase was slightly less in the CAPs-exposed group but the difference in slopes was not statistically significant. Measurements of ECG parameters at night were initiated in the second month of the study. Heart rates at night were significantly higher than during the day, which is typical for the diurnal pattern of rodents. The air-exposed mice also exhibited a heart rate increase during the exposure; the rate of increase, as indicated by the slope of the dashed blue line, was nearly identical with the slope of the change observed during the day (solid blue line). However, the CAPs-exposed mice did not exhibit any heart rate increase over time when measured at night (dashed red line). It is reasonable to expect that the increased buildup of arterial plaque in the mouse's arteries would engender an increased rate of heart rate to compensate for the more restricted blood flow. To that extent the failure of the heart of the CAPs-exposed mice to compensate for the plaque buildup could be an indication of an adverse effect.

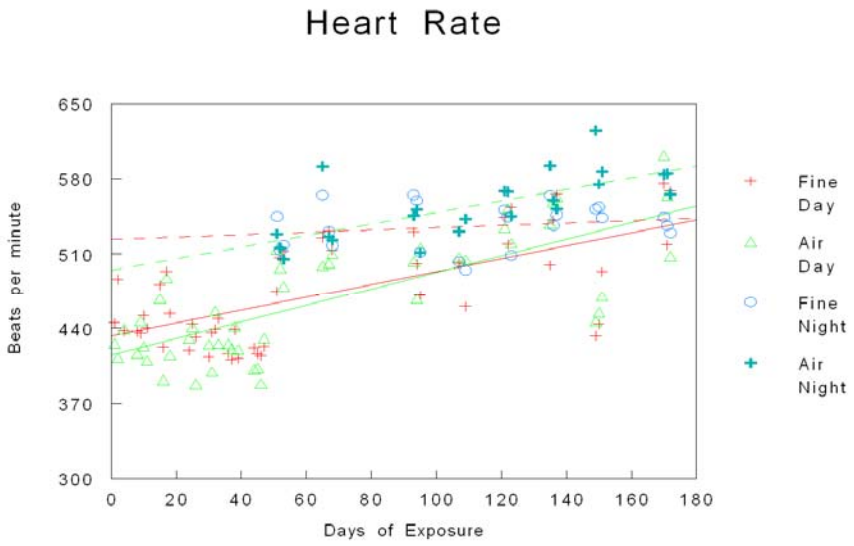

Figure 6. Heart Rates in Mice During and After Exposure During a 6-month Study

Heart rate variability (HRV), measured as the standard deviation of the normal R to R interval, was assessed from the ECG data. As shown in Figure 7, this measurement was very unstable and although there were minor differences between exposure groups, only the diurnal changes were of statistical significance. The data for power analysis are available and will be evaluated in the future. A power analysis approach could possibly identify whether there is a change in sympathetic vs. parasympathetic pathway balance as a result of exposure.

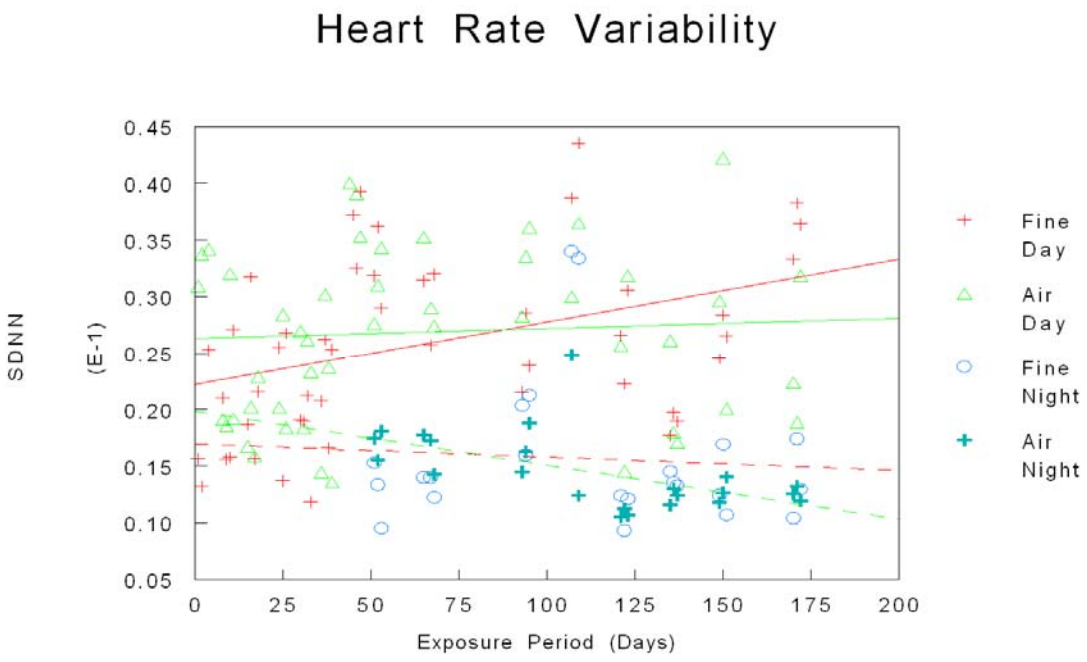

Figure 7. Changes in Heart Rate Variability During a 6-month Study

ECG tracings were evaluated for abnormal heart beats (arrhythmias) and for wave forms suggestive of cardiac ischemia. A normal ECG tracing is shown in Figure 8. Loss of oxygen delivery to the heart muscle because of arterial occlusion results in changes in polarization and repolarization. In our system this can be observed as ST segment depression or elevation.

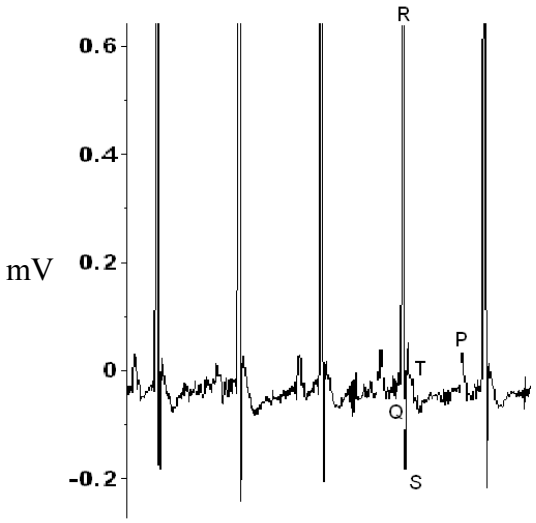

Figure 8. Normal ECG Tracing Showing Typical P,Q,R,S and T Waveform

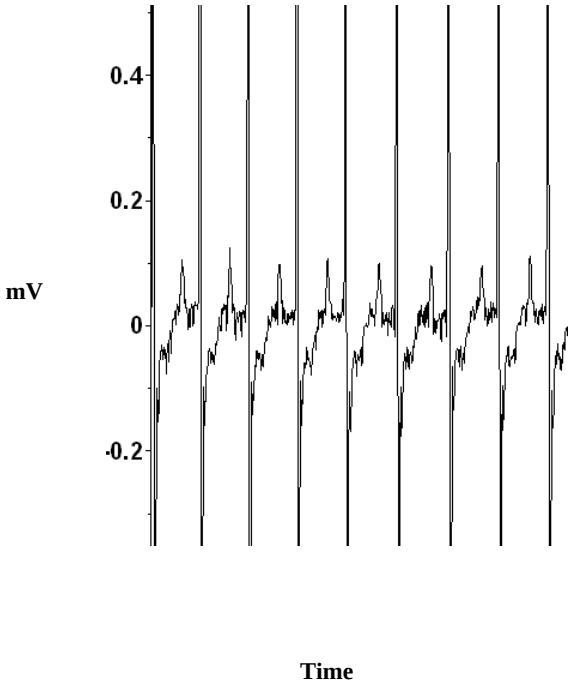

Figure 9. ECG from CAPs-exposed Mouse Showing ST-segment Depression

Ischemia was seen in air-exposed mice as well as in CAPs-exposed mice. These data were tabulated in terms of the number of days per month in which abnormal ECGs were

seen over the same 5 minute period each day and normalized to the number of days in that month for which 'clean', artifact-free tracings were obtained and expressed as a fraction. The results are summarized in Figure 10. The control group had a higher initial rate of abnormal tracings at the beginning of the study and the rate decreased progressively with time. The mice were not initially matched with respect to ECG abnormalities. Both groups had periods of abnormal heart beats which may be related to their genetically induced impaired lipid metabolism. The number of abnormal ST events in the CAPs-exposed group did not change with time ($r^2 = 0.10$; n.s.) over the measurement period, whereas the number of ST changes in the control group significantly decreased over the experiment period ($r^2 = 0.68$; $p = 0.044$). The number of data points analyzed during the last month (November) was lower than in the prior months because the study ended midmonth, hence the uncertainty around those values is greater, as indicated by the relatively large error bars.

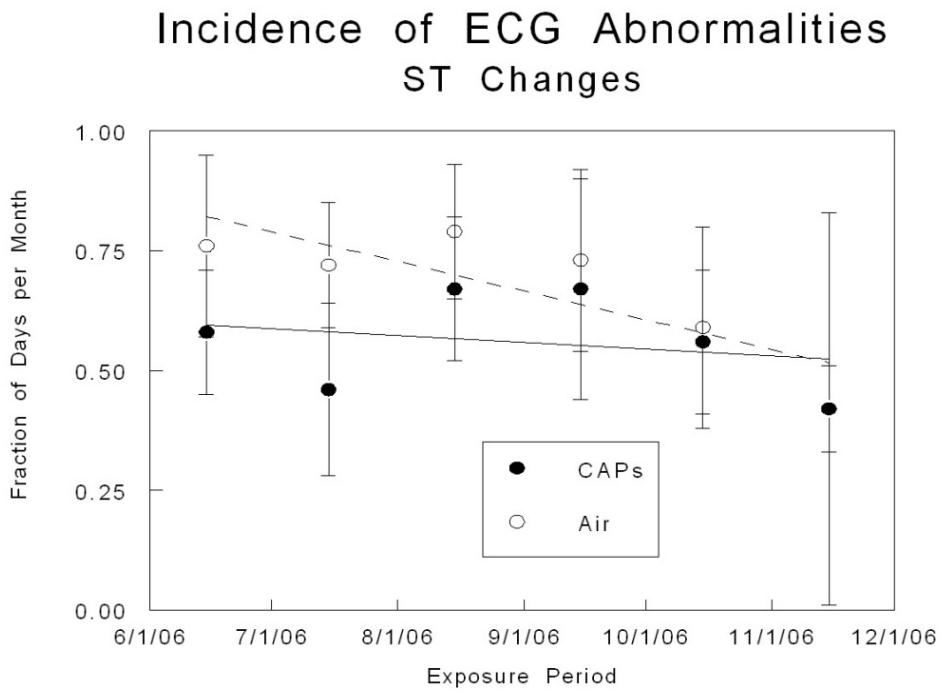

Figure 10. Changes in the ratio of numbers of days in a monitoring month with ST abnormalities compared to the total number of monitoring days for that month.

Biomarkers of Systemic and Vascular Inflammation

These studies were performed with mice that were genetically prone to have abnormal lipid metabolism resulting in high levels of circulating lipids. We have used a custom assay set that analyzed protein biomarkers associated with vascular inflammation and oxidative stress. Data were obtained for: plasminogen activation inhibitor-1 (PAI-1), which is an acute-phase reactant that can become transiently elevated by inflammation and plays a role in atherothrombosis; soluble forms of the intercellular, vascular and

endothelial cell adhesion molecules ICAM-1, VCAM-1 and E-selectin, that are postulated to play a role in development of atherosclerotic plaque; matrix metallopeptidase-9 which is involved in tissue remodeling associated with inflammatory disease processes; and C-reactive protein, which is produced in the liver and is an acute phase proteins that increase during systemic inflammation. These data are summarized in Table 5. There was a significant increase of MMP-9 in the CAPs-exposed mice. Soluble E-selectin was slightly increased and the difference with the air-exposed group mean value approached significance.

Table 5. Biomarkers of Systemic and Vascular inflammatory Processes (ng/mL Plasma)

Biomarker	Air (n = 16)	Caps (n = 16)	P value
PAI-1	n.d.	n.d.	--
s-VCAM	1050 ± 45	980 ± 57	n.s.
s-ICAM	25 ± 2	27 ± 3	n.s.
s-E Selectin	12 ± 3	17 ± 3	$p \leq 0.1$
MMP-9	31 ± 7	56 ± 9	$p = 0.03$ *
CRP	24 ± 2	23 ± 1	n.s.

n.d. – non-detect; n.s. – not significant; *statistically significant

Although the indications of inflammation in the aortal tissue were only slightly more elevated in the samples from exposed vs control mice, we attempted to determine whether there was more oxidative stress in tissues from the CAPs-exposed group than the air-exposed group. To accomplish this we measured protein carbonyls and malonaldehyde (MDA) in extracts from homogenized tissues of the aortal arch and the descending aorta. There were no significant differences for MDA in either tissue (data not shown), but protein carbonyls are a more specific indicator of oxidant injury to

tissues than the more commonly used MDA (or TBARs) determinations. We analyzed frozen specimens from the aorta arch and from the thoracic region of the descending aorta. In apoE-/- mice plaque is generally seen in the arch region but not in the thoracic region, hence we hypothesized that we would expect to more evidence of oxidative injury in the arch than in the thoracic samples. The data are summarized in Table 6. We found no significant differences in the content of protein carbonyls between samples from the aortic arch vs. the thoracic region of the aorta and there were no significant effects of exposure. The levels seen in the apoE-/- mice were slightly greater than those seen in wild type mice (Wang et al. 2006).

Table 6. Protein Carbonyls in Aortal Tissue

Sample Location	Arch (n = 8)	Thoracic Region (n = 8)
Air	8.4 ± 0.8	8.1 ± 0.4
CAPs	7.3 ± 0.5*	8.2 ± 0.4

*One outlier removed from data set

It is not necessarily surprising that the inflammatory and oxidative stress biomarkers are similar between the groups since there was significant plaque development in both air-exposed and CAPs-exposed mice. We therefore examined how one of the markers related to plaque formation using the plasma levels of CRP and the ultrasound measurement of arterial plaque measured after 4 months of exposure. These data are shown in Figure 11.

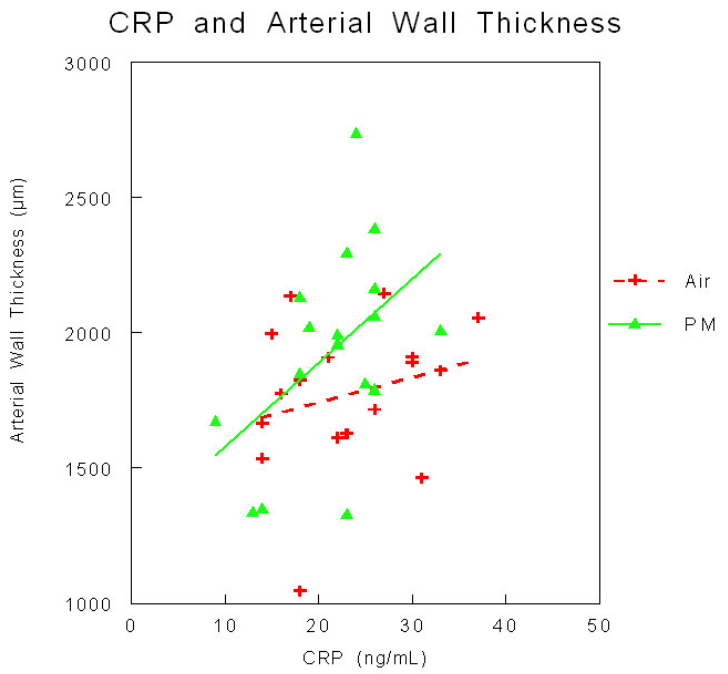

Figure 11. Relationship between Plaque Formation Measured Ultrasonically and Plasma CRP (n=16/group)

As seen in Figure 11, there is a linear relationship between plasma CRP and plaque formation for the CAPs-exposed mice. The slope of the relationship is greater for the mice exposed to CAPs (r^2= 0.25; $p \leq 0.05$) than for the mice exposed to filtered air (r^2 = 0.06; n.s.). Thus, although the group averages of CRP concentrations were not different in the air and CAPs-exposed groups, for the same concentration of CRP (i.e. for the same level of systemic inflammation) the CAPs-exposed mice developed more plaque. This finding supports the use of CRP as a biomarker for atherogenic risk and also suggests that air pollution if it is not a direct causative factor in the atherosclerotic process, may be a potentiator of adverse health effects.

Summary of NYU Findings (Sun et al. 2005)

ApoE-/- mice were, based on randomized assignments, fed with normal chow or high-fat chow and exposed to CAP (concentrated $PM_{2.5}$) or filtered air (FA) in Tuxedo, NY, for 6 hours per day, 5 days per week for a total of 6 months. In the high-fat chow group, the mean (SD) composite plaque area of CAPs vs FA was 41.5% ± 9.8% vs 26.2% ± 8.6%, respectively (P<.001); and in the normal chow group, the composite plaque area was 19.2% ± 13.1% vs 13.2% ± 8.1%, respectively (P = .15). Lipid content in the aortic arch measured by oil red-O staining revealed a 1.5-fold increase in mice fed the high-fat chow and exposed to CAPs vs FA (30.0 ± 8.2 vs 20.0 ±7.0; 95% confidence interval [CI], 1.21-1.83; P = .02). Vasoconstrictor responses to phenylephrine and serotonin challenge in the thoracic aorta of mice fed high-fat chow and exposed to CAPs were exaggerated compared with exposure to FA (mean ± SE, 134.2% ± 5.2% vs 100.9% ± 2.9%, for phenylephrine, and 156.0% ± 5.6% vs 125.1% ± 7.5%, for serotonin; both P = .03); relaxation to the endothelium-dependent agonist acetylcholine was attenuated (mean ± SE of half-maximal dose for dilation, 8.9 ± 0.2 x 10-8 vs 4.3 ± 0.1 x 10-8, respectively; p = 0.04). Mice fed high-fat chow and exposed to CAPs demonstrated marked increases in macrophage infiltration, expression of the inducible isoform of nitric oxide synthase, increased generation of reactive oxygen species, and greater immunostaining for the protein nitration product 3-nitrotyrosine (all $p \leq 0.001$). They concluded that in an apoE-/- mouse model, long-term exposure to CAPs altered vasomotor tone, induced vascular inflammation, and potentiated atherosclerosis.

Conclusions

The primary results of this study are that: (1) subchronic exposure to elevated concentrations of $PM_{2.5}$ can potentiate the development of atherosclerosis; (2) $PM_{2.5}$ exposure may alter cardiovascular physiology; (3) these changes occurred in the absence

of evidence of significant pulmonary inflammation; and (4) C-reactive protein is a useful biomarker that is associated with the development of atherosclerotic plaques.

An earlier study performed by colleagues at NYU also showed that CAPs exposure accelerated the development of atherosclerotic plaques. An important difference between our findings and those of NYU was that we demonstrated significant potentiation of atherosclerosis in mice fed a standard chow diet whereas the NYU group showed significant changes only in mice fed a high fat diet. While it is possible that Los Angeles PM, which is greatly influenced by motor vehicle emissions, might be more toxic, or atherogenic, than the PM used in the NY study which was more influenced by aged, regional PM, there were several protocol differences between the studies that should be considered. The particle concentrations used in our study were greater on the average than those used in the NYU study (166 $\mu g/m^3$ vs 85 $\mu g/m^3$), there may have been stresses induced by the transportof mice during our study, and the total exposure time per week was 24 hr in our study compared to 30 hr for the NYU study. We therefore cannot definitively determine that LA PM is more atherogenic than NY PM primarily because dose may have been a critical factor.

We also present evidence that the concentration of C-reactive protein in plasma may be a useful biomarker for systemic inflammation associated with development of atherosclerosis. Although the group averages of CRP concentrations were not different in the air and CAPs-exposed groups, for the same concentration of CRP (i.e. for the same level of systemic inflammation) the CAPs-exposed mice developed more plaque. This finding supports the use of CRP as a biomarker for atherogenic risk and also suggests that air pollution, if it is not a direct causative factor in the atherosclerotic process, may be a potentiator of adverse health effects.

We noted that heart rate increased over the 6-month exposure period of this study in the mice exposed to purified air. It is reasonable to expect that the increased buildup of arterial plaque in the mouse's arteries would engender an increased rate of heart rate to compensate for the more restricted blood flow. However, the CAPs-exposed mice did

not exhibit an increased heart rate (i.e. this compensation was blunted). It is possible that the failure of the cardiac physiology of the CAPs-exposed mice to compensate for the plaque buildup by increasing the heart rate could be an indication of an adverse effect.

It is important to note that the blunting of the normal compensation of the cardiovascular system for the reduced lumen area due to plaque formation and the increased rate of plaque formation that we observed in the PM-exposed mice were not associated with significant inflammation in the lungs. It is possible that after the 6 month exposure period the pulmonary system of the mice had compensated for the inflammatory effects of PM. It is possible, however, that some subtle changes that we have not measured could have occurred. For example it is possible that there might be changes in the lung parenchymal collagen, as has been seen after chronic O_3 exposure. The lung tissue that we have preserved from these animals can be analyzed in the future to look for these and other subtle indicators of pulmonary injury.

In this study, both control and PM-exposed groups had periods of abnormal heart beats monitored by their ECGs which may have been related to their genetically induced impaired lipid metabolism. The mice were not initially matched with respect to ECG abnormalities and the control group had a higher initial rate of abnormal tracings at the beginning of the study. The number of abnormal events in the control group decreased progressively, and significantly ($r^2 = 0.68$; $p = 0.044$), over the 6 months of the study. The number of abnormal ST events in the CAPs-exposed group did not change with time ($r^2 = 0.10$; n.s.). If the groups had been matched initially on the ECG parameter, it is possible that the results would have shown an increase in ECG abnormalities in the PM-exposed mice.

Although there were some methodological differences between our study and that conducted by NYU we found that the PM in Riverside CA significantly potentiated plaque development in mice fed a normal diet whereas this was not the case in the NYU study. We are presently attempting to do a more direct comparison of the potency of PM from CA vs. the PM from several other cities with markedly different source contribution

profiles. It is hypothesized that this follow-on study, which is funded by the Health Effects Institute, will allow us to identify specific sources or components of PM that are closely associated with the acceleration of plaque formation and may contribute to cardiac mortality.

This study has important implications for California residents and for the Air Resources Board. It confirms that PM exposure can contribute to development of atherosclerosis. Although this is an animal study using genetically modified mice that have abnormal lipid metabolism, the mice in this study were on normal diets and it has been reported that under these conditions the mice have high values of total cholesterol (400 to 500) but these are levels that may be seen in some humans. Like many humans with untreated cardiovascular disease these mice have a much higher ratio of low density lipoproteins to high density lipoproteins (LDL/HDL ratio). Thus the results of this study should be considered to be relevant to humans and suggest that air pollution exposure is a preventable contributor to human health risks in California.

References:

Campen MJ, Nolan JP, Schladweiler MC, Kodavanti UP, Evansky PA, Costa DL, et al. 2001. Cardiovascular and thermoregulatory effects of inhaled PM-associated transition metals: a potential interaction between nickel and vanadium sulfate. Toxicol Sci 64(2): 243-252.

Carter JD, Ghio AJ, Samet JM, Devlin RB. 1997. Cytokine production by human airway epithelial cells after exposure to an air pollution particle is metal-dependent. Toxicol Appl Pharmacol 146(2): 180-188.

Chang MC, Geller MD, Sioutas C, Fokkens PHB, Cassee FR. 2002. Development and evaluation of a compact, highly efficient coarse particle concentrator for toxicological studies. Aerosol Sci Tech 36(4): 492-501.

Ghio AJ, Stonehuerner J, Dailey LA, Carter JD. 1999. Metals associated with both the water-soluble and insoluble fractions of an ambient air pollution particle catalyze an oxidative stress. Inhal Toxicol 11(1): 37-49.

Hlavay J, Polyak K, Weisz M. 2001. Monitoring of the natural environment by chemical speciation of elements in aerosol and sediment samples. J Environ Monit 3(1): 74-80.

Kim S, Chang MC, Kim D, Sioutas C. 2000a. A new generation of portable coarse, fine, and ultrafine particle concentrators for use in inhalation toxicology. Inhalation Toxicology 12: 121-137.

Kim S, Jaques PA, Chang MC, Barone T, Xiong C, Friedlander SK, et al. 2001a. Versatile aerosol concentration enrichment system (VACES) for simultaneous in vivo and in vitro evaluation of toxic effects of ultrafine, fine and coarse ambient particles - Part II: Field evaluation. Journal of Aerosol Science 32(11): 1299-1314.

Kim S, Jaques PA, Chang MC, Froines JR, Sioutas C. 2001b. Versatile aerosol concentration enrichment system (VACES) for simultaneous in vivo and in vitro evaluation of toxic effects of ultrafine, fine and coarse ambient particles - Part I: Development and laboratory characterization. Journal of Aerosol Science 32(11): 1281-1297.

Kim S, Sioutas C, Chang MC, Gong H. 2000b. Factors affecting the stability of the performance of ambient fine-particle concentrators. Inhalation Toxicology 12: 281-298.

Kleeberger SR, Reddy S, Zhang LY, Jedlicka AE. 2000. Genetic susceptibility to ozone-induced lung hyperpermeability: role of toll-like receptor 4. Am J Respir Cell Mol Biol 22(5): 620-627.

Kleinman MT, Hamade A, Meacher D, Oldham M, Sioutas C, Chakrabarti L, et al. 2005. Inhalation of concentrated ambient particulate matter near a heavily trafficked road stimulates antigen-induced airway responses in mice. Journal of the Air & Waste Management Association 55(9): 1277-1288.

Lippmann M, Ito K, Hwang JS, Maciejczyk P, Chen LC. 2006. Cardiovascular effects of nickel in ambient air. Environmental Health Perspectives 114(11): 1662-1669.

Maciejczyk P, Zhong M, Li Q, Xiong J, Nadziejko C, Chen LC. 2005. Effects of subchronic exposures to concentrated ambient particles (CAPs) in mice. II. The design of a CAPs exposure system for biometric telemetry monitoring. Inhal Toxicol 17(4-5): 189-197.

Magari SR, Schwartz J, Williams PL, Hauser R, Smith TJ, Christiani DC. 2002. The association of particulate air metal concentrations with heart rate variability. Environ Health Perspect 110(9): 875-880.

Morokata T, Ishikawa J, Ida K, Yamada T. 1999. C57BL/6 mice are more susceptible to antigen-induced pulmonary eosinophilia than BALB/c mice, irrespective of systemic T helper 1/T helper 2 responses. Immunology 98(3): 345-351.

Natusch DFS, Wallace JR, Evans CA. 1974. Toxic Trace-Elements - Preferential Concentration in Respirable Particles. Science 183(4121): 202-204.

Ohtsuka Y, Clarke RW, Mitzner W, Brunson K, Jakab GJ, Kleeberger SR. 2000. Interstrain variation in murine susceptibility to inhaled acid-coated particles. American Journal of Physiology-Lung Cellular and Molecular Physiology 278(3): L469-L476.

Oldham MJ, Phalen RF, Robinson RJ, Kleinman MT. 2004. Performance of a portable whole-body mouse exposure system. Inhal Toxicol 16(9): 657-662.

Rouse RL, Murphy G, Boudreaux MJ, Paulsen DB, Penn AL. 2008. Soot nanoparticles promote biotransformation, oxidative stress, and inflammation in murine lungs. Am J Respir Cell Mol Biol 39(2): 198-207.

Sioutas C, Kim S, Chang M. 1999. Development and evaluation of a prototype ultrafine particle concentrator. J Aerosol Sci 30(8): 1001-1017.

Sun Q, Wang A, Jin X, Natanzon A, Duquaine D, Brook RD, et al. 2005. Long-term air pollution exposure and acceleration of atherosclerosis and vascular inflammation in an animal model. Jama 294(23): 3003-3010.

Sun Q, Yue P, Deiuliis JA, Lumeng CN, Kampfrath T, Mikolaj MB, et al. 2009. Ambient air pollution exaggerates adipose inflammation and insulin resistance in a mouse model of diet-induced obesity. Circulation 119(4): 538-546.

Wang Y, Feinstein SI, Manevich Y, Ho YS, Fisher AB. 2006. Peroxiredoxin 6 gene-targeted mice show increased lung injury with paraquat-induced oxidative stress. Antioxid Redox Signal 8(1-2): 229-237.